FEBS Open Bio 4 (2014) 407–419

FEBS openbio

journal homepage: www.elsevier.com/locate/febsopenbio

CK2 phosphorylation of human centrins 1 and 2 regulates their binding to the DNA repair protein XPC, the centrosomal protein Sfi1 and the phototransduction protein transducin β

Dora Grecu, Liliane Assairi *

Institut Curie-Centre de Recherche, F-91405 Orsay Cédex, France
Institut National de la Santé et de la Recherche Médicale (INSERM) U759, F-91405 Orsay Cédex, France

ARTICLE INFO

Article history:
Received 12 February 2014
Revised 10 April 2014
Accepted 10 April 2014

Keywords:
Centrins
XPC
Sfi1
Transducin
CK2

ABSTRACT

Centrins are calcium-binding proteins that can interact with several cellular targets (Sfi1, XPC, Sac3 and transducin β) through the same hydrophobic triad. However, two different orientations of the centrin-binding motif have been observed: $W^1xxL^4xxxL^8$ for XPC (xeroderma pigmentosum group C protein) and the opposite orientation $L^8xxxL^4xxW^1$ for Sfi1 (suppressor of fermentation-induced loss of stress resistance protein 1), Sac3 and transducin β. Centrins are also phosphorylated by several protein kinases, among which is CK2. The purpose of this study was to determine the binding mechanism of human centrins to three targets (transducin β, Sfi1 and XPC), and the effects of in vitro phosphorylation by CK2 of centrins 1 and 2 with regard to this binding mechanism. We identified the centrin-binding motif at the COOH extremity of transducin β. Human centrin 1 binds to transducin β only in the presence of calcium with a binding constant lower than the binding constant observed for Sfi1 and for XPC. The affinity constants of centrin 1 were 0.10 10^6 M^{-1}, 249 10^6 M^{-1} and 52.5 10^6 M^{-1} for Trd, R17-Sfi1 and P17-XPC respectively. CK2 phosphorylates human centrin 1 at residue T138 and human centrin 2 at residues T138 and S158. Consequently CK2 phosphorylation abolished the binding of centrin 1 to transducin β and reduced the binding to Sfi1 and XPC. CK2 phosphorylation of centrin 2 at T138 and S158 abolished the binding to Sfi1 as assessed using a C-HsCen2 T138D-S158D phosphomimetic form of centrin 2.

1. Introduction

The EF-hand superfamily is primarily composed of calmodulin, and centrins, which are small Ca^{2+}-binding proteins. Centrins were first identified in the unicellular green algae, *Tetraselmis striata* [1] and *Chlamydomonas reinhardtii* [2] and are conserved proteins. However, although lower eukaryotes such as unicellular algae and yeast, possess only one centrin, higher eukaryotes possess several isoforms that are generated by either gene duplication or retrotransposition from messenger RNA. These isoforms can integrate into the chromosome as demonstrated by murine Cen1 [3] and Cen4; in some cases, isoforms have been reduced to pseudogenes, such as in humans [4,5]. Centrins are composed of two relatively independent EF-hand domains with each domain containing two EF-hand motifs that bind Ca^{2+}. Although the two Ca^{2+}-binding sites located within the C-terminal domain are functional, the Ca^{2+}-binding sites in the N-terminal domain may not be functional, depending on the organism.

Centrins are localized to the centrosomes [6] and spindle pole bodies in *Saccharomyces cerevisiae* [7]. Centrin 2 is ubiquitously expressed, but centrin 1 expression is restricted to ciliated cells, such as retinal photoreceptor cells [8]. Currently at least five centrin-targets are known: XPC (xeroderma pigmentosum group C protein), which has 1 centrin-binding site and, is involved in DNA repair [9]; Sfi1 (suppressor of fermentation-induced loss of stress resistance protein 1), which is a helicoid protein, has 25 centrin-binding motifs and is involved in centrosome duplication and cellular division [10]; Sac3 which is involved in RNA transfer from

Abbreviations: C-HsCen, C-terminal domain of centrin; CK2, casein protein kinase; HPLC, high pressure liquid chromatography; HsCen, human centrin; ITC, isothermal titration calorimetry; MALDI-TOF, matrix-assisted laser desorption ionization time of flight; Sfi1, suppressor of fermentation-induced loss of stress resistance protein 1; Trd, transducin; XPC, xeroderma pigmentosum group C protein

* Corresponding author at: Institut Curie, Centre de Recherche, INSERM U759, 15 Rue Georges Clemenceau, Centre Universitaire d'Orsay, Bâtiment 112, F-91405 Orsay Cédex, France. Tel.: +33 169863178; fax: +33 169075327.
E-mail address: liliane.assairi@curie.u-psud.fr (L. Assairi).

http://dx.doi.org/10.1016/j.fob.2014.04.002
2211-5463/

the nucleus to the cytoplasm [11]; Kar1 which is located on the spindle pole bodies [12]; and transducin which is a G-protein involved in the phototransduction cascade [13,14]. In all cases, centrin binds its targets through a hydrophobic triad $W^1xxL^4xxxL^8$ that was originally identified in XPC. However, in other centrin targets, such Sac3 and Sfi1, the triad is in the reverse orientation $L^8xxxL^4xxW^1$.

Two crystal structures of integral human centrin 2 in complex with a 17-residue peptide derived from the human XPC [15,16] and one crystal structure of yeast centrin Cdc31 in complex with two or three repeats of *S. cerevisiae* Sfi1 [17] have been solved by X-ray crystallography. From these structures, the residues involved in the interaction between centrin and its targets have been determined, and the F113 residue of human centrin was identified as the critical residue necessary to bind its targets (XPC and Sfi1) through several contacts, especially with the W^1 residue of the centrin-targets.

Solution structures of centrin in apo form [18] as well as in complex with either XPC [19] or Sfi1 [20] have also been resolved using NMR. Because the helix dipoles of XPC and Sfi1 are in opposing orientations, the consequences of helix dipole orientation were analyzed after the superimposition of the two NMR structures of human centrin 2 in complex with either XPC or with Sfi1. For both structures, the W residue of the triad is similarly embedded in the cavity where the centrin F113 residue is situated. However, for Sfi1, this implies a rotation of the W residue, which is accompanied by a slight translation of the movement along the peptide helix axis toward centrin 2. Owing to this movement the E148 residue, which contacts XPC, is pushed out and is no longer able to contact Sfi1.

Transducin is another centrin target that has been analyzed at the cellular level; however, no structural study of the transducin–centrin complex has yet been conducted. Two transducin β isoforms are found in the retina: transducin β1 is expressed in rods and transducin β3 is expressed in cones. Experiments using immunoelectron microscopy have shown that centrin and transducin co-localize in the connecting cilium of rod photocells in mice, and co-immunoprecipitation studies and centrifugation and size-exclusion chromatography experiments have demonstrated that transducin β and the heterotrimer transducin αβγ bind to centrin 1 [13]. The four isoforms of murine centrin have different subcellular localizations. Cen1, 2, and 3 are found in the connecting cilium although both Cen2 and Cen3 are found in the basal body whereas Cen4 is only located in the basal body [14,21].

The heterotrimeric G proteins (αβγ) transduce and amplify external signals. When GDP is bound to Gα it leads to the association of Gα with the two other subunits βγ. Furthermore, G protein-coupled signaling is regulated by two mechanisms. The first is the intrinsic GTPase activity of $G_t\alpha$, by which $G_t\alpha$ GTP is inactivated and reassociates with $G_t\beta\gamma$. Second, phosducin binds $G_t\beta\gamma$ thereby blocking its association: with $G_t\alpha$. Phosducin was first found in retina extracts but has since been shown to be expressed in various tissues [22,23]. The structure of phosducin in complex with transducin βγ has been solved using X-ray crystallography [24,25]. The binding of phosducin to transducin βγ is regulated by the phosphorylation of the S73 residue of phosducin by PKA. Phosphorylated phosducin then releases transducin β which then reassociates with transducin α [26].

In vertebrate photoreceptor cells, centrins are phosphorylated by the casein kinase CK2 in a light-dependent manner; this allows CK2 to co-localize with the centrins in the inner lumen of the connecting cilium. As a consequence of phosphorylation, the centrins have reduced affinities for transducin [27]. CK2 has been shown to phosphorylate murine centrin at T138, which is increased during the dark adaptation of photoreceptor cells and leads to the reduced binding of centrin to transducin. After illumination, the dephosphorylation of centrins by the PP2C-α and β phosphatases [28] results in increased binding to transducin. The transport of these proteins between the outer and inner segments at the ciliary junctions of photoreceptor cells is also light-dependent. This information, in addition to the large Ca^{2+} variations in these cells, suggests that Ca^{2+} may be involved in the transport of these proteins during the phototransduction cascade.

Because the centrin-binding motifs on XPC and both Sfi1 and transducin β have an opposing orientation, we investigated the effect of this inversion on the binding reaction. We also analyzed the effect of phosphorylation of centrin on its binding to targets based on the binding-motif orientation. The thermodynamics of the binding of human centrin 1 to transducin β was assessed using microcalorimetry and compared to the binding of other centrin targets (XPC, Sfi1). We report here that centrin 1 binds transducin β exclusively in the presence of Ca^{2+}, but with a lower affinity than that of centrin for its other targets XPC and Sfi1. A detailed study using transducin β variants allowed us to determine which residues were responsible for this lower binding affinity. We also report that the phosphorylation of centrin 1 by CK2 regulates its binding to transducin β. Additionally, we observed that CK2 phosphorylates human centrin 2 at T138 and S158 and consequently regulates centrin 2 binding to Sfi1 and XPC.

2. Results

2.1. CK2 phosphorylates centrin 1 on T138 and centrin 2 at T138 and S158

Both human centrins 1 and 2 (C-terminal domain including residues M93 to Y172) have been shown to be phosphorylated by the protein kinase CK2 (catalytic α and regulatory β subunits complex). Consequently, one phosphorylated form of centrin 1 was generated, but two phosphorylated forms of centrin 2 were identified by HPLC chromatography (Fig. S1A). The chromatograms show that the phosphorylated centrin 1 was the only protein observed after 24 h. Diphosphorylated centrin 2 was the primary form observed after 24 h. The determination of the phosphorylated residues was assessed using MALDI-TOF mass spectrometry of trypsinized fragments of both C-HsCentrins 1 and 2. It was observed that CK2 phosphorylated centrin 1 on T138 and centrin 2 on T138 and S158.

The sequences of centrins 1 and 2 differ by only three residues (Fig. 1). The centrin 1 amino acids N131, N158, and E160 are replaced by K131, S158, and Q160 in centrin 2. The T138 residue is present in both centrins and surrounded by following three acidic residues: D139, E140, and E141, which constitute the signature of a CK2 phosphorylation site. The S158 residue is only found in centrin 2 and is also surrounded by two acidic residues E159 and E161.

T138 residue is located within an unstructured loop between the two α-helices F (residues 124–132) and G (residues 139–149), and the three acidic residues (D139, E140, E141) are located at the extremity of the α-helix G. S158 is located at the junction of calcic loop IV and α-helix H (residues 159–166), and the acidic residues (E159, E161) are located at the extremity of the α-helix H (Fig. S1B, C).

2.2. Residue 131 is responsible for the different phosphorylation rates between centrins 1 and 2

The kinetics of CK2 phosphorylation on the C-terminal domains (M93-Y172) of both centrins 1 (C-HsCen1) and 2 (C-HsCen2) were performed in parallel in the presence of either EGTA or Ca^{2+} (Fig. 1A and B). First, the two isoforms exhibited a different phosphorylation rate; after 3 h at 37 °C, 62% of the C-HsCen1 protein was phos-

```
HsCen1      MASGFKKPSAASTGQKRKVAPKPELTEDQKQEVREAFDLFDVDGSGTIDAKELKVAMRAL
HsCen2      MASNFKKANMASSSQRKRMSPKPELTEEQKQEIREAFDLFDADGTGTIDVKELKVAMRAL
HsCen3      MSLALRSELLVDKTKRKKRR---ELSEEQKQEIKDAFELFDTDKDEAIDYHELKVAMRAL
            *:  ::.   ... ::::     **:*:****:::**:***.*   :** :*********

HsCen1      GFEPRKEEMKKMISEVDREGTGKISFNDFLAVMTQKMSEKDTKEEILKAFRLFDDDETGK
HsCen2      GFEPKKEEIKKMISEIDKEGTGKMNFGDFLTVMTQKMSEKDTKEEILKAFKLFDDDETGK
HsCen3      GFDVKKADVLKILKDYDREATGKITFEDFNEVVTDWILERDPHEEILKAFKLFDDDDSGK
            **: :* :: *::.: *:*.***:.* **  *:*: : *:*.:*******:*****::**

HsCen1      ISFKNLKRVANELGENLTDEELQEMIDEADRDGDGEVNEEEFLRIMKKTSLY
HsCen2      ISFKNLKRVAKELGENLTDEELQEMIDEADRDGDGEVSEQEFLRIMKKTSLY
HsCen3      ISLRNLRRVARELGENMSDEELRAMIEEFDKDGDGEINQEEFIAIMTGDI--
            **::**:***.*****::****: **:* *:*****.::**: **.
```

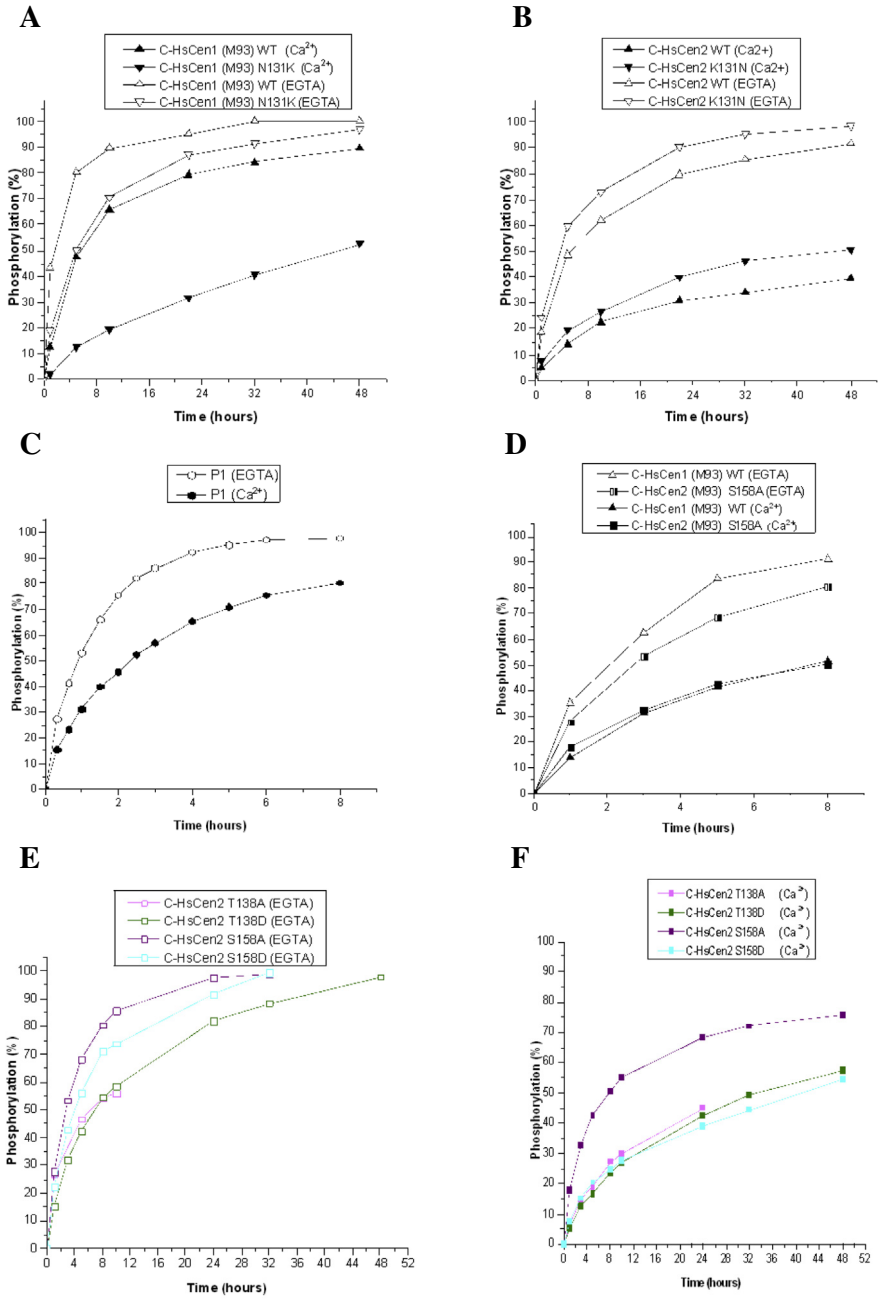

Fig. 1. Phosphorylation of human centrins 1 and 2 by CK2. Human centrins are aligned using ClustalW program. The sequence analysis shows (∗) identity, (:) strongly similar, (.) weakly similar residues. Amino acids are colored in green based on their implication in target binding, in red based on their phosphorylation potentiality. (A, B) The phosphorylation rate is higher for HsCen1 than for HsCen2. Effect of Ca^{2+} and implication of the residue 131, on the CK2 access. (C) Ca^{2+} inhibits the CK2 activity as assessed using a peptide containing the CK2 signature. (D) Phosphorylation of T138 residue of C-HsCen1 and C-HsCen2. (E, F) Effect of a phosphorylated residue on the phosphorylation of a second residue. All the kinetics were carried out using the CK2 complex composed of catalytic α and regulatory β subunits. The phosphorylation rate was determined by the quantification of phosphorylated and unphosphorylated forms of centrin after integrating peaks identified by HPLC separation. In the case of C-HsCen2, the phosphorylation % corresponded to the sum of the two peaks identified on HPLC chromatograms. For each graph, the experiments were run in parallel. (For interpretation of the references to color in this figure legend, the reader is referred to the web version of this article.)

phorylated, but only 45% of the C-HsCen2 protein was phosphorylated. The presence of Ca^{2+} reduced the phosphorylation rate to 30% and 15% for centrins 1 and 2, respectively; 95% of the C-HsCen1 protein was phosphorylated after 10 h in the presence of EGTA, but such a level was only achieved after 48 h in the presence of Ca^{2+}.

Both HsCen1 and HsCen2 have a different residue at position 131; this residue is N131 in centrin 1 and K131 in centrin 2. Residue 131 is on the surface of the protein and most likely interacts with CK2; therefore, the K-131 residue could reduce the ability of CK2 to access centrin (Fig. S1C). This hypothesis was assessed using site-directed mutagenesis (C-HsCen1-N131K and C-HsCen2-K131N). The N131K mutation reduced the phosphorylation of centrin 1 by 30% after 5 h (80% HsCen1 wild type vs. 50% C-HsCen1N131K) (Fig. 1A). The addition of Ca^{2+} reduced the phosphorylation of centrin 1 by 30% and 40% for C-HsCen1 and C-HsCen1-N131K, respectively.

The situation was reversed in the case of centrin 2; the K131N mutation resulted in an increase in phosphorylation by 12% (48% for C-HsCen2 wild-type vs. 60% for C-HsCen2-K131N) after 5 h (Fig. 1B). Because the level of phosphorylation corresponded to the sum of the two sites (T138 and S158), the weak increase in phosphorylation that was observed demonstrated that the K131 residue had an inhibitory effect on the phosphorylation of the T138 residue, but not on that of the S158 residue. The presence of Ca^{2+} also resulted in a reduction in phosphorylation at the same extent for the wild type and for the K131N C-HsCen2 proteins. Ca^{2+} also had an effect on the S158 residue, which is located at the base of the calcium loop IV.

2.3. Ca^{2+} inhibits CK2 activity

The peptide "WELGENTDEELQEMID", which is derived from centrin 1, contains the T138 residue surrounded by the acidic residues that comprise the CK2 phosphorylation site. We tested the capacity of such a peptide to be phosphorylated by CK2. First, we observed that the peptide was phosphorylated. The presence of Ca^{2+} inhibited its phosphorylation by approximately 20% to 25%, and 80% of the peptide was phosphorylated at 8 h (Fig. 1C). However, Ca^{2+} reduced the phosphorylation of C-HsCen1 by 30% and 80% of the protein was phosphorylated after 48 h (Fig. 1A). The inhibitory effect of Ca^{2+} was more evident in the case of centrin 2, where only 50% of the protein was phosphorylated after 48 h (Fig. 1B). Thus, Ca^{2+} reduced CK2 kinase activity by acting on the kinase itself, and Ca^{2+} also induced changes in the conformation of centrin, which in turn led to a reduction in its phosphorylation. Because this phenomenon is more important for centrin 2, we concluded that the S158 residue is most likely more sensitive to Ca^{2+}.

2.4. Relationship between the T138 and S158 phosphorylated residues

By mutating the C-HsCen2 S158 residue to alanine, we reduced the phosphorylation sites to the unique site T138. We observed that the rate of phosphorylation of C-HsCen2 T138 was lower than of C-HsCen1 T138 (Fig. 1D). We investigated the rate of CK2 phosphorylation at both T138 and S158 on C-HsCen2. Using the S158A variant, we determined the rate of phosphorylation of the T138 residue; conversely, using the T138A variant, we determined the phosphorylation of the S158 residue. Under these conditions, we observed that the T138 residue exhibited a 20% increase of the phosphorylation rate compared with the S158 residue (Fig. 1E and F).

The presence of Ca^{2+} reduced the phosphorylation rate of both T138 and S158 but the reduction at S158 was more prominent by a factor of 2.7 compared with the reduction at T138 which was a factor of 1.8.

We also investigated the effect of phosphorylation by CK2 at one site on the phosphorylation at the other site (Fig. 1E and F). The phosphomimetic mutation T138D had no effect on the rate of phosphorylation of S158 even in the presence of Ca^{2+}. However, the C-HsCen2-S158D exhibited a reduced phosphorylation rate at T138 by a factor of 1.36, and the presence of Ca^{2+} increased this reduction by a factor of 2.1.

2.5. Human centrin 1 binds transducin β whose hydrophobic triad has a specific composition

The three human transducin β isoforms (β1, code P62873; β2, code P62879; β3, code P16520) are composed of 340 amino acids and contains seven WD repeats; the final WD repeat (M_{325}AVATGSWDSFLKIWN$_{340}$) is identical for the three isoforms and is located at the C-terminus. This specific WD repeat was designated as a potential centrin-binding target based on comparisons to the Sfi1 and XPC motifs. We analyzed the capacity of centrin to bind one of the seven WD motifs (S_{74}QDGKLIIWDSYTTNKV$_{90}$) of transducin β1 (Fig. S2) (Fig. S5), and observed that this peptide did not bind centrin (Fig. S2). We further analyzed the capacity of C-HsCen1 to bind the transducin β-derived peptide (MAVATGSWDSFLKIWN$_{340}$), which appeared to have the potential to bind to centrin. We observed that this peptide bound centrin but only in the presence of Ca^{2+} (Fig. 2). The binding reaction occurred with an exothermic heat exchange (negative enthalpy) and a 1:1 stoichiometry. The experimental data could be best fit into a one-site binding model with an equilibrium association constant $K_a = 0.54\ 10^6\ M^{-1}$. We observed the same binding behavior using the full-length centrin 1 (Fig. 3), and Ca^{2+} was absolutely required for the binding of transducin β1, but the binding constant was weak ($K_a = 0.17\ 10^6\ M^{-1}$).

R18-Sfi1 showed an affinity weaker than XPC in the presence of EDTA (Fig. 2). Reversing the sequence orientation of R17-Sfi1, (R17-Sfi1inv Table 1), increased its affinity for centrin 1 by nearly 10-fold in the absence of Ca^{2+}. This mutation also increased the change in enthalpy (ΔH: −43 kcal/mole to −26 kcal/mole), which was accompanied by an increase in the change in entropy ($T\Delta S$: −36 kcal/mole to −18.42 kcal/mole) (Table 2).

Several peculiarities were observed for the centrin-binding site of transducin β. These included the unusual presence of W332 at position 8 of the hydrophobic triad and the presence of the acidic residue D333 at position 7, where a basic residue is usually found in other centrin targets. Two point mutations, W332L and D333R, were analyzed (Table 2). The W332L mutation did not significantly change the affinity of Trd for C-HsCen1, which was similar to what was observed for full-length centrin 1. The Trd-D333R variant showed a small increase in affinity for centrin. However, the double mutation (Trd-W332L-D333R) increased the affinity of transducin β for centrin by almost a factor of 100 in the presence of Ca^{2+} (Table 2). Additionally, binding of TrdW332L-D333R to C-HsCen1 occurred in the presence of EDTA with an affinity constant of $0.1\ 10^6\ M^{-1}$ which is only 5-fold lower than the affinity constant observed for wild type transducin β in the presence of Ca^{2+} ($0.54\ 10^6\ M^{-1}$). We also observed an increase in the change in enthalpy by a factor of 2 for the double mutant as well as an increase in the affinity. Thus, the double mutation W332L-D333R has a centrin binding behavior similar to Sfi1.

2.6. Phosphorylation at the T138 residue of centrin 1 abolishes the binding of transducin β

CK2 phosphorylation of centrin 1 at T138 abolished its ability to bind transducin β (Fig. 3). Additionally, the T138D phosphomimetic mutation had no effect on the binding of centrin 1 to transducin β whereas direct phosphorylation by CK2 did. However, the

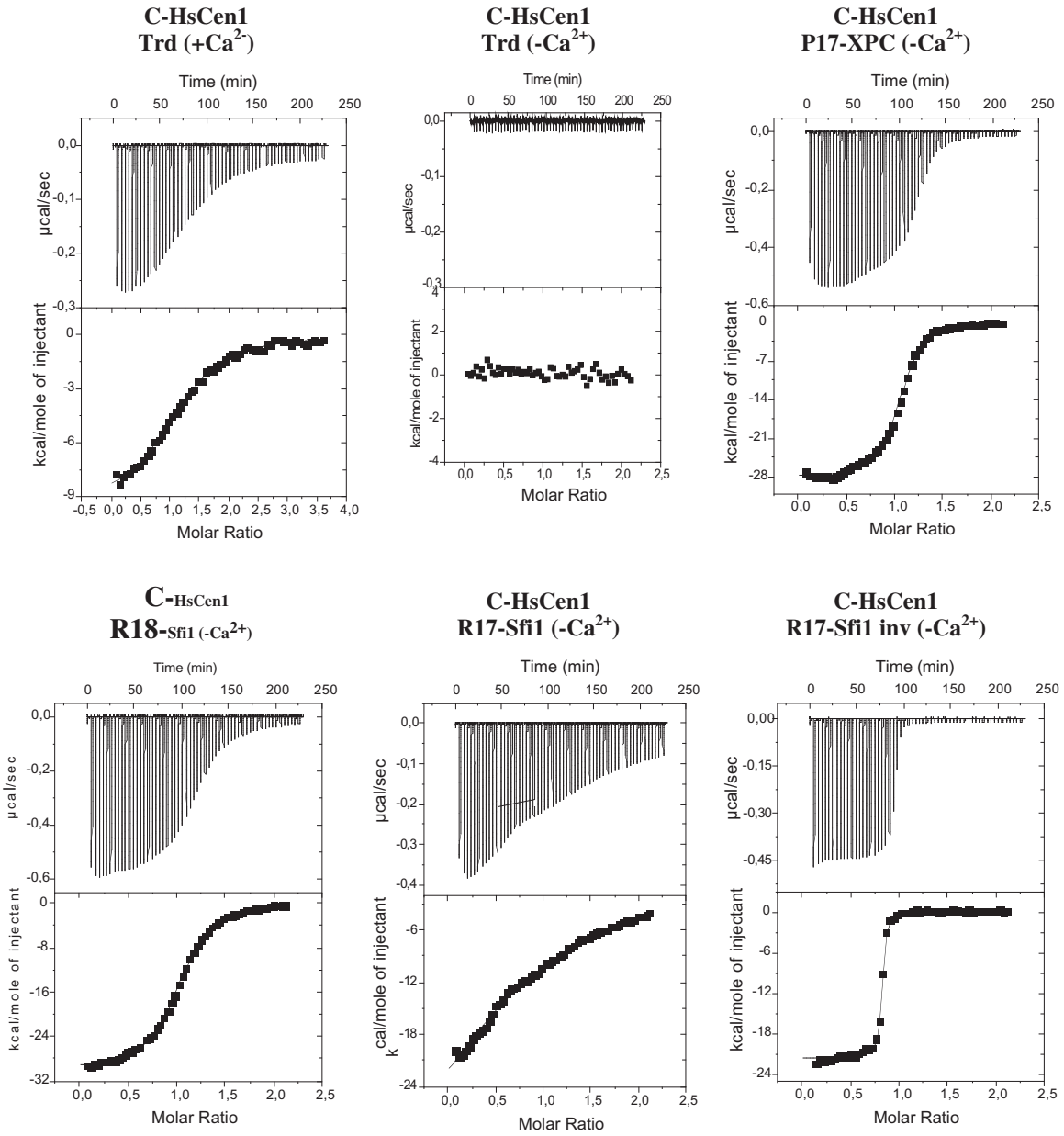

Fig. 2. Effect of the orientation of the centrin-binding motif on the target binding to C-HsCen1 as measured by ITC. The ITC measurements show the C-HsCen1 binding to several targets: Trd β (centrin-binding motif), P17-XPC, R18-Sfi1, R17-Sfi1, and R17-Sfi1 inv. The upper panels show the raw data, and the lower panels show the binding isotherms fitted to a one-site model. Peptide solutions (100 µM) were injected into the protein (10 µM) equilibrated in buffer (MOPS 50 mM, NaCl 100 mM, EDTA 2 mM or $CaCl_2$ 1 mM, pH 7.5) at 30 °C in the calorimeter cell.

entropy (ΔS) was increased by a factor of 8 and the change in free energy (ΔG) remained constant; also, the change in enthalpy (ΔH) increased by a factor of 5, resulting in a less negative and therefore less favorable value (Table 3). Glutamate residues have longer side chains than aspartate residues, and are more similar to phosphoserines; however, aspartate is more similar to unphosphorylated serine. Because threonine residues are longer than serine residues, glutamate is the best candidate to mimic the phosphorylation of a threonine residue. Therefore, the second variant T138E was constructed only for the C-terminal domain for HsCen1 (C-HsCen1-T138E), and this mutation more efficiently mimicked the phosphorylation than the C-HsCen1-T138D construct. The results show that the T138E mutation decreased the affinity of centrin 1 for transducin β by a factor of 7 (Fig. S3).

Because the transducin motif contains a W residue at position 8, which is commonly occupied by an L residue in other centrin targets (XPC and Sfi1), we also used the mutated transducin β peptide $W^{332}L$. This mutated peptide showed results similar to the wild type Trd- (Table 3). Thus, there was no binding between the transducin β-derived peptide and centrin 1, which was phosphorylated by CK2. However, HsCen1-T138D still bound to the transducin β $W^{332}L$ peptide with a binding constant reduced by half with similar enthalpy and entropy changes.

2.7. Phosphorylation at T138 of centrin 1 has a weak effect on centrin binding to XPC

XPC is a protein consisting of 940 amino acids and contains only one centrin-binding hydrophobic triad $W^{848}xxL^{851}xxxL^{855}$, which is located at the C-terminus. However, this motif is in the opposite orientation compared to the centrin-binding motif found in transducin β.

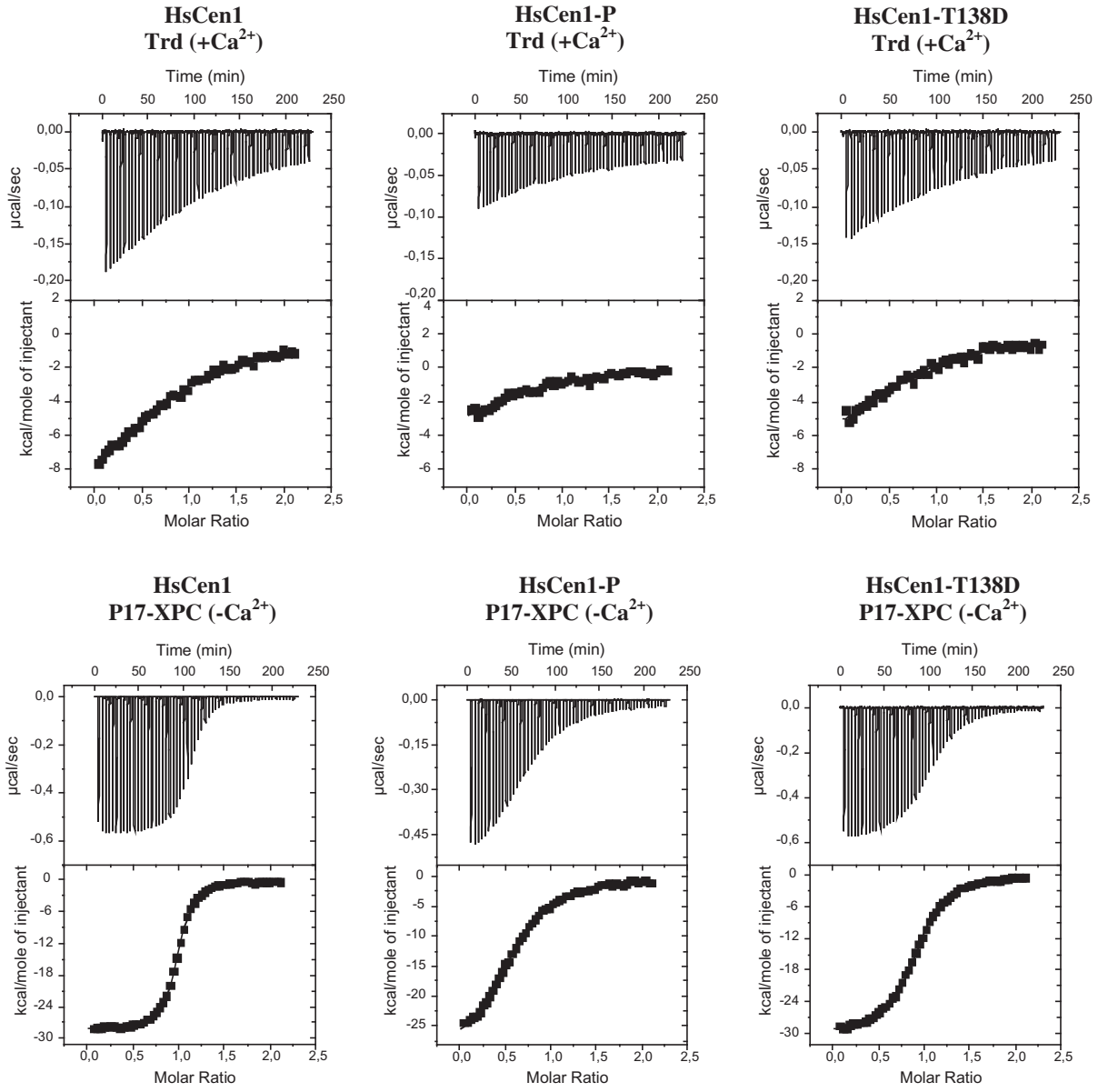

Fig. 3. Regulation by CK2 phosphorylation of the centrin 1 binding to tranducin β and to P17-XPC as measured by ITC. The ITC measurements show the Trd and XPC binding to centrin 1 (unphosphorylated, phosphorylated centrin, and T138D phosphomimetic). For each graph, the upper panels show the raw data, and the lower panels show the binding isotherms fitted to a one-site model. Peptide solutions (100 µM) were injected into the protein (10 µM) equilibrated in buffer (MOPS 50 mM, NaCl 100 mM, EDTA 2 mM or $CaCl_2$ 1 mM, pH 7.5) at 30 °C in the calorimeter cell.

Table 1
Peptides used for ITC experiments.

HsTrBWD:	74-SQDGKLIIWDSYTTNKV-90
HsTrB:	325-MAVATGSWDSFLKIWN-340
HsTrBW332L:	325-MAVATGSLDSFLKIWN-340
HsTrBD333R:	325-MAVATGSWRSFLKIWN-340
HsTrBW332L-D333R:	325-MAVATGSLRSFLKIWN-340
HsSfiR18:	677-SQHNRQLLRGALRRWK-692
HsSfiR17:	641-RADLHHQHSVLHRALQAWVT-660
HsSfilR17inv:	660-TVWAQLARHLVSHQHHLDAR-641
P17-XPC :	846-NWKLLAKGLLIRERLKR-863
CEN1P[a]:	W131-ELGENLTDEELQEMID-147

[a] A tryptophan residue was added at the N-terminus for UV measurement.

Contrary to transducin β, the binding of centrin to XPC did not require Ca^{2+}, although the presence of Ca^{2+} increased the binding by a factor of 5 (Table 3). Phosphorylation at T138 reduced binding to XPC in the presence of EDTA by a factor of 10 (Fig. 3). The T138D phosphomimetic mutation reduced the binding to XPC by a factor of 4 in the presence of EDTA (Fig. 3). However, the T138D mutation did not completely mimic the phosphorylation. Therefore, we investigated the second C-HsCen1-T138E, and this mutation more efficiently mimicked the phosphorylation compared with the C-HsCen1-T138D construct (Fig. S3). The T138E mutation decreased the affinity of centrin 1 for XPC by a factor of 20 in the presence of EDTA, whereas the T138D mutation decreased the affinity for XPC by a factor of 2. However, the enthalpy was unchanged, and the entropy slightly increased to 4 kcal/mole in the presence of EDTA, leading to a reduction in free energy by 2 kcal/mole.

Contrary to transducin β, phosphorylation of centrin 1 at T138 weakly affected XPC binding. The centrin-binding motif of both XPC and transducin β are in opposite orientations, and this situation is most likely the cause for the centrin-specific phosphorylation effect observed.

Table 2
Thermodynamic parameters of C-HsCen1 binding to Trd, P17-XPC, R17- and R18-Sfi1.

Protein	Ligand	Ca^{2+}	N	K_a (error) (10^6 M^{-1})	ΔH (error) (kcal/mol)	$T\Delta S$ (kcal/mol)	ΔG (kcal/mol)
C-HsC1	Trd	+	1.2	0.54 (0.3)	−9.57 (0.13)	−1.62	−7.95
		–	NB	NB	NB	NB	NB
C-HsC1	P17-XPC	+	0.93	39.6 (0.15)	−23.27 (0.05)	−12.73	−10.54
		–	1.05	8.25 (4.3)	−28.1 (0.13)	−18.57	−9.53
C-HsC1	R18-Sfi1	+	0.99	81.5 (78)	−22.5 (0.087)	−11.51	−10.99
		–	1.03	3.56 (1.3)	−29.8 (0.12)	−20.75	−9.05
C-HsC1	R17-Sfi1	+	1.21	125 (126)	−18.0 (0.06)	−6.79	−11.21
		–	0.88	0.12 (0.09)	−43.1 (2.6)	−36.06	−7.04
C-HsC1	R17inv-Sfi1	+	0.80	149 (142)	−21.57 (0.08)	−10.21	−11.36
		–	0.825	0.69 (0.3)	−26.55 (0.34)	−18.42	−8.13
C-HsC1	TrdW332L	+	0.85	0.85 (0.8)	−13.82 (0.03)	−5.57	−8.25
		–	NB	NB	NB	NB	NB
C-HsC1	TrdD333R	+	1.2	1.7 (0.5)	−12.09 (0.06)	−3.42	−8.67
		–	NB	NB	NB	NB	NB
C-HsC1	TrdW332L-D333R	+	0.94	20 (9.3)	−18.93 (0.06)	−8.82	−10.11
		–	1.19	0.10 (0.09)	−9.8 (0.64)	−2.82	−6.15

The ITC experiments were conducted at 30 °C in buffer (MOPS 50 mM, NaCl 100 mM, EDTA 2 mM or $CaCl_2$1 mM, pH 7.5). N was the stoichiometry of binding. The standard deviations of the fitted parameters are given in parenthesis.

Table 3
Thermodynamic parameters of HsCen1 and C-HsCen1 binding to Trd, P17-XPC, R17- and R18-Sfi1.

Protein	Ligand	Ca^{2+}	N	K_a (error) (10^6 M^{-1})	ΔH (error) (kcal/mol)	$T\Delta S$ (kcal/mol)	ΔG (kcal/mol)
HsC1	Trd	+	0.83	0.17 (0.12)	−12.23 (0.5)	−4.97	−7.26
		–	NB	NB	NB	NB	NB
HsC1P	Trd	+	NB	NB	NB	NB	NB
		–	NB	NB	NB	NB	NB
HsC1T138D	Trd	+	0.75	0.18 (0.26)	−8.14 (0.7)	−0.85	−7.29
		–	NB	NB	NB	NB	NB
C-HsC1	Trd	+	1.2	0.54 (0.3)	−9.57 (0.013)	−1.62	−7.95
		–	NB	NB	NB	NB	NB
C-HsC1T138D	Trd	+	1.15	0.2	−9.97(0.4)	−2.62	−7.35
C-HsC1T138E	Trd	+	1.18	0.073	−10.0(0.4)	−3.03	−6.97
HsC1	TrdW332L	+	0.78	0.13 (0.13)	−10.6 (0.8)	−3.5	−7.1
		–	NB	NB	NB	NB	NB
HsC1P	TrdW332L	+	NB	NB	NB	NB	NB
		–	NB	NB	NB	NB	NB
HsC1T138D	TrdW332L	+	0.76	0.06 (0.15)	−12.16 (3.7)	−5.5	−6.66
		–	NB	NB	NB	NB	NB
HsC1	P17-XPC	+	1.04	52.5 (23)	−28.44 (0.08)	17.72	−10.72
		–	0.98	12.2 (2.7)	−28.43 (0.05)	18.6	−9.83
HsC1P	P17-XPC	+	0.58	46.2 (25)	−34.57 (0.11)	−23.94	−10.63
		–	0.61	0.84 (0.24)	−30.45 (0.27)	−22.21	−8.24
HsC1T138D	P17-XPC	+	0.95	102 (103)	−28.47 (0.11)	−17.36.21	−11.11
		–	0.92	2.9 (0.6)	−30.17 (0.08)	−21.18	−8.99
C-HsC1	P17-XPC	+	0.93	39.6 (0.15)	−23.27 (0.05)	−12.73	−10.54
		–	1.05	8.25 (4.3)	−28.1 (0.13)	−9.57	−9.53
C-HsC1T138D	P17-XPC	+	0.86	33.4 (1.9)	−23.6 (0.07)	−13.18	−10.43
		–	0.93	4.55 (0.12)	−30.19 (0.08)	−20.93	−9.26
C-HsC1T138E	P17-XPC	+	1.01	9.03 (0.83)	−21.22 (0.16)	−11.57	−9.65
		–	0.93	0.43 (0.02)	−32.56 (0.61)	−24.72	−7.84
HsC1	R18-Sfi1	+	0.88	249 (345)	−35.49 (0.14)	−23.81	−11.68
		–	0.88	3.47 (0.7)	−34.70 (0.09)	−25.66	−9.04
HsC1P	R18-Sfi1	+	0.65	85.6 (78)	−39.40 (0.16)	−28.48	−10.92
		–	0.57	0.258 (0.1)	−42.96 (1.60)	−35.45	−7.51
HsC1T138D	R18-Sfi1	+	0.77	239 (307)	−36.73 (0.14)	−25.09	−11.64
		–	0.83	0.875 (0.2)	−36.44 (0.20)	−28.18	−8.26
HsC1	R17-Sfi1	–	1.12	0.347 (0.2)	−19.25 (0.37)	−11.57	−7.68
HsC1P	R17-Sfi1	–	NB	NB	NB	NB	NB

The ITC experiments were conducted at 30 °C in buffer (MOPS 50 mM, NaCl 100 mM, EDTA 2 mM or $CaCl_2$1 mM, pH 7.5). N was the stoichiometry of binding. NB means no binding. The standard deviations of the fitted parameters are given in parenthesis.

2.8. Phosphorylation of centrin 1 at T138 reduced its binding to Sfi1

We investigated the effects of centrin 1 phosphorylation on ability to bind to human Sfi1, another centrin target that is 1242 amino acids in length. Sfi1 contains 25 centrin-binding sites, which are in the same orientation as the centrin-binding site of transducin β. Similarly to P17-XPC, R18-Sfi1 (Table 1), bound to centrin 1 in the absence of Ca^{2+} (Fig. 4), although the presence of Ca^{2+} did increase its binding. The binding reaction took place with an exothermic heat exchange (negative enthalpy) and a 1:1 stoichiometry; the one-site binding model gave an equilibrium association constant $K_a = 3.5\ 10^6\ M^{-1}$ and $2.5\ 10^8\ M^{-1}$ in the absence and presence of Ca^{2+}, respectively (Table 3). Phosphorylation of centrin 1 at T138 reduced the ability of the protein to bind to R18-Sfi1 by a factor of 10 in the absence or in the presence of Ca^{2+}.

Because HsSfi1 has 25 homologous but not identical centrin-binding sites, we also investigated another Sfi1-repeat, R17-Sfi1

(Table 1) (Fig. 4). The binding constant of HsCen1 to R17-Sfi1 decreased by a factor of 10 in the absence of Ca^{2+} compared with R18-Sfi1 (Table 3). The change in enthalpy was reduced and accompanied by an increase in entropy by a factor of 2. Phosphorylation at T138 abolished the binding of centrin 1 to R17-Sfi1 in the absence of Ca^{2+}.

2.9. The T138D and S158D phosphomimetics of centrin 2 exhibited reduced binding to XPC

The effect of the two T138D and S158D single mutations (Fig. S4) as well as the T138D-S158D double mutation on binding of centrin 2 to XPC was analyzed in the absence of Ca^{2+} (Fig. 5). The T138D mutation reduced the affinity for P17-XPC by a factor of 3 and increased the negative enthalpy by a factor of 1.7; the S158D mutation reduced the affinity for XPC by a factor of 3.7 but the enthalpy stayed the same. However, the T138D-S158D double mutation reduced the affinity by a factor of 9 and slightly increased the negative enthalpy. Clearly, phosphorylation at S158 acted in concert with phosphorylation at T138 to reduce the binding of centrin 2 to P17-XPC. However, the T138D-S158D double mutation did not completely abolish the binding of centrin 2 to P17-XPC.

In the presence of Ca^{2+} (Table 4), the T138D mutation reduced affinity of centrin 2 to XPC by a factor of 2 but the S158D mutation exhibited a smaller reduction of the affinity. The T138D-S158D double mutation reduced the affinity for XPC by a factor of 2 as the T138D mutation. The three variants exhibited an identical enthalpy and entropy.

2.10. The T138D-S158D phosphomimetic of centrin 2 does not bind to R17-Sfi1 in the absence of Ca^{2+}

In the absence of Ca^{2+} (Fig. S4), the T138D phosphomimetic mutation had no effect on the affinity to R17-Sfi1 but induced a strong decrease of the negative enthalpy and a strong decrease of the negative entropy because of the unfavorable binding. The

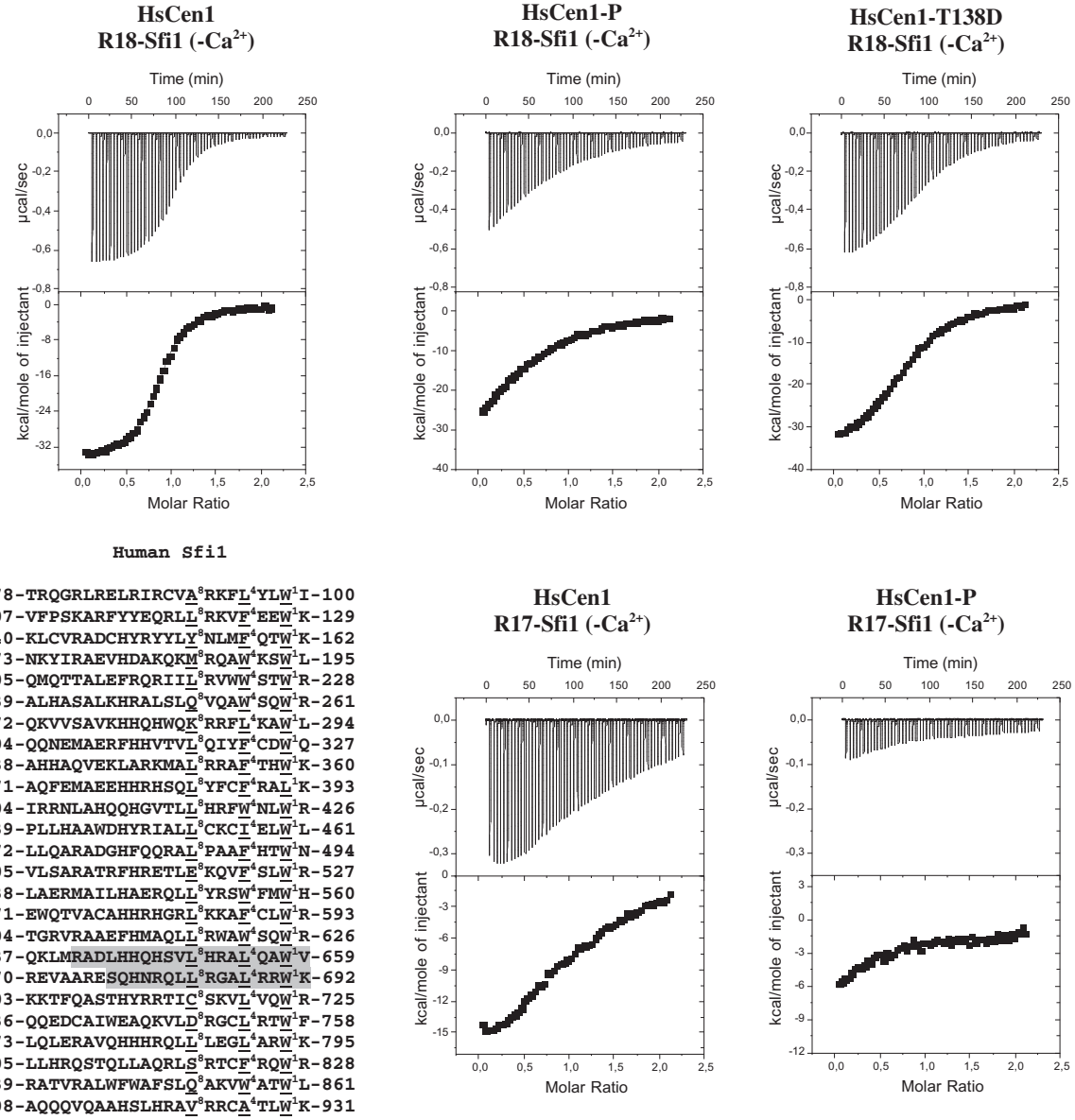

Fig. 4. Regulation by CK2 phosphorylation of the centrin 1 binding to Sfi1 as measured by ITC. The ITC measurements show the HsCen1 (unphosphorylated, phosphorylated centrin and T138D phosphomimetic) binding to R18-Sfi1 and R17-Sfi1. The upper panels show the raw data, and the lower panels show the binding isotherms fitted to a one-site model. Peptide solutions (100 µM) were injected into the protein (10 µM) equilibrated in buffer (MOPS 50 mM, NaCl 100 mM, EDTA 2 mM, pH 7.5) at 30 °C in the calorimeter cell. Human Sfi1 centrin-binding motifs, the residues composing the hydrophobic triad are underlined (bottom left).

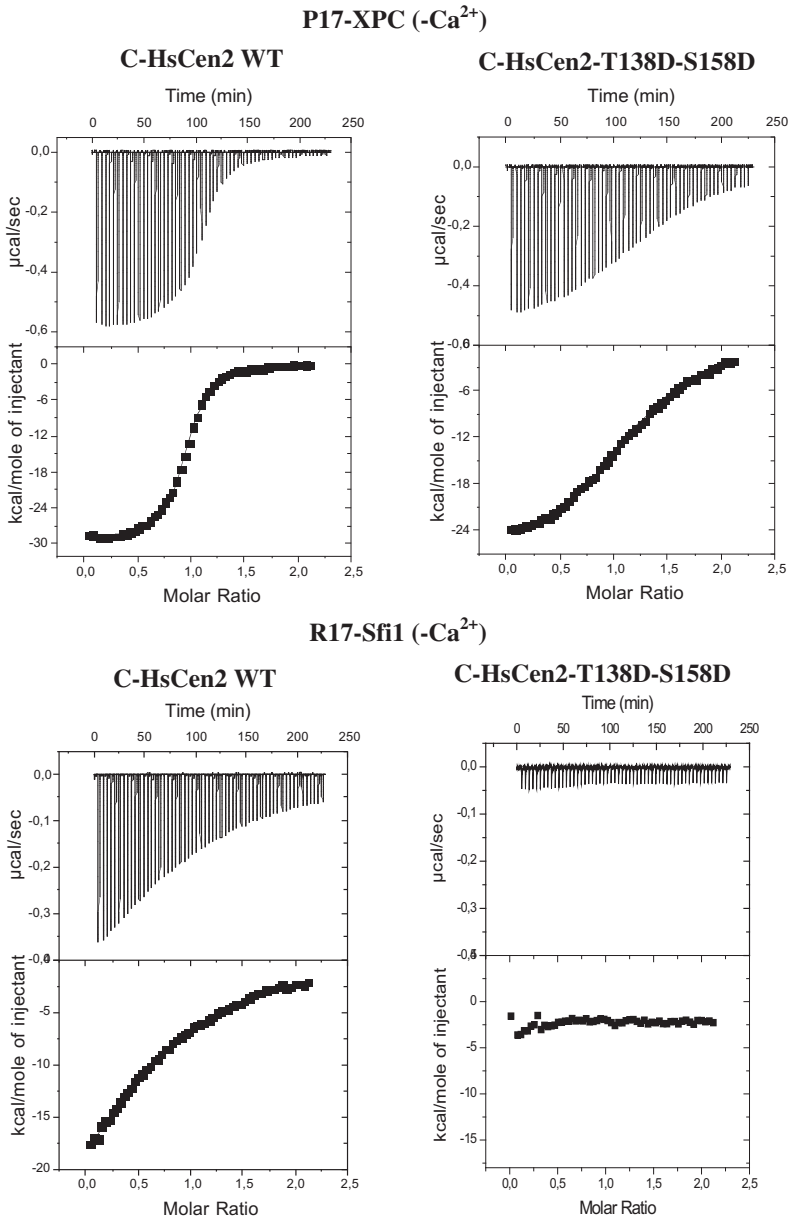

Fig. 5. Regulation by CK2 phosphorylation of the centrin 2 binding to P17-XPC and R17-Sfi1 as measured by ITC. The ITC measurements show the HsCen2 (unphosphorylated and T138D-S158D phosphomimetic) binding to P17-XPC and R17-Sfi1. The upper panels show the raw data, and the lower panels show the binding isotherms fitted to a one-site model. Peptide solutions (100 µM) were injected into the protein (10 µM) equilibrated in buffer (MOPS 50 mM, NaCl 100 mM, EDTA 2 mM, pH 7.5) at 30 °C in the calorimeter cell.

S158D mutation reduced the affinity by a factor of 4.7 with an almost identical enthalpy, but the negative entropy increased as a consequence of unfavorable binding. In contrast to XPC, the T138D-S158D double mutation abolished the binding of centrin 2 to R17-Sfi1 (Fig. 5).

In the presence of Ca^{2+} (Table 4), the T138D mutation increased the affinity for R17-Sfi1 by a factor of 3, and the S158D mutation increased the affinity by a factor of 5; both of these variants had an enthalpy almost identical to the wild type protein under similar conditions. The S158D mutation increased the affinity by a factor of 5 with an almost identical enthalpy. The T138D-S158D double mutation increased the affinity by a factor of 2 with the same enthalpy. For the three variants, the negative entropy increased by a factor of 2.

3. Discussion

3.1. Centrins bind several targets the centrin-binding motif of which exists in the two orientations

An important feature of the interaction between centrin and its targets is that the centrin-binding motif exists in both orientations (i.e., WxxLxxxL for XPC and LxxxLxxW for Sfi1, transducin β and Sac3). The NMR structures of C-HsCen2 in complex with either the XPC-derived peptide [19] or Sfi1-derived peptide [20] showed that the E148 residue binds XPC but not Sfi1. Further site-directed mutagenesis of the homologue of the E144 residue from the *Scherffelia dubia* illustrated this target specificity [29].

Table 4
Thermodynamic parameters of C-HsCen2 binding to P17-XPC and R17-Sfi1.

Protein C-HsC2	Ligand	Ca^{2+}	N	K_a (error) (10^6 M^{-1})	ΔH (error) (kcal/mol)	$T\Delta S$ (kcal/mol)	ΔG (kcal/mol)
WT	P17-XPC	+	0.81	52.7(2.3)	−23.4(0.06)	−12.7	−10.7
		−	0.95	7.35(0.2)	−29.3(0.09)	−19.75	−9.55
T138D	P17-XPC	+	0.82	27.1(1.7)	−24(0.09)	−13.7	−10.31
		−	0.94	2.5(0.04)	−32.7(0.08)	−23.88	−8.82
S158D	P17-XPC	+	0.89	43.1(1.9)	−23(0.05)	−12.63	−10.37
		−	1.181.0.7	2.02(0.1)	−23.8(0.03)	−15.03	−8.77
T138D-S158D	P17-XPC	+	1.18	29.0(1.7)	−23.9(0.08)	−13.6	−10.3
		−		0.8(0.02)	−26.8(0.15)	−18.6	−8.2
WT	R17-Sfi1	+	0.95	18.2(0.8)	−20.2(0.06)	−6.12	−14.08
		−	0.72	0.19(0.0)	−31.3(0.09)	−23.97	−7.33
T138D	R17-Sfi1	+	0.86	45.4(2.1)	−24.3(0.06)	−13.66	−10.64
		−	0.75	0.23(0.04)	−9.76(0.09)	−2.31	−7.45
S158D	R17-Sfi1	+	0.7	101(7.3)	−25.9(0.008)	−14.76	−11.14
		−	0.77	0.04(0.01	−38.5(22.3)	−32.12	−6.38
T138D-S158D	R17-Sfi1	+	0.91	35(2.6)	−22.4(0.09	−11.88	−10.52
		−	NB	NB	NB	NB	NB
			0.91	24.9(0.9)	−20.15(0.05)	−9.94	−10.21
WT	R17inv	+	1.09	0.36(0.03)	−21.96(0.7)	−14.24	−7.72

The ITC experiments were conducted at 30 °C in buffer (MOPS 50 mM, NaCl 100 mM, EDTA 2 mM or $CaCl_2$1 mM, pH 7.5). N was the stoichiometry of binding. The standard deviations of the fitted parameters are given in parenthesis.

3.2. Three targets (XPC, Sfi1 and transducin β) bind centrin with various affinities and different levels of Ca^{2+}-dependence

A centrin-binding site was identified in the C-terminus of transducin β, and it was recorded as the last WD motif. We recognized the characteristic hydrophobic triad of the centrin-binding motif, and tested this triad for centrin binding using ITC; we also tested the binding of centrin to another WD motif found in transducin β and observed no interaction. By contrast, the last WD motif was observed to bind centrin exclusively in the presence of Ca^{2+}, although its affinity was lower than the affinity observed for other centrin targets (XPC and Sfi1). Interactions between murine centrins and transducin have previously been demonstrated by co-immunoprecipitation and centrifugation assays [13]. Here, we corroborated these results and showed that human centrins also bind to transducin β. Moreover, using the ITC method, we assessed the mechanism of interaction between centrin and transducin β at the molecular level. Some peculiarities were observed with transducin β. First, centrin had a very weak binding affinity for transducin β. The observed K_a was 0.15 10^6 M^{-1}, 249 10^6 M^{-1} and 52.5 10^6 M^{-1} for Trd, R17-Sfi1 and P17-XPC respectively. Additionally, the presence of Ca^{2+} was absolutely required for this interaction to occur. The presence of a W residue in position 8 of the hydrophobic triad is unusual compared to the other centrin-targets that is, XPC, Sfi1, and Sac3. Indeed, among the 25 centrin-binding motifs identified in human Sfi1, none of these motifs has a W residue at position 8. However, a W residue at position 4 can be found in 7 centrin-binding motifs in human Sfi1 (Fig. S5). The presence of an acidic residue, such as D, in place of the basic R residue at position 7 is also unusual, though this substitution is strongly conserved among GNB proteins (Fig. S2).

3.3. Phosphorylation of human centrins 1 and 2 by CK2

CK2 is a serine/threonine protein kinase; however, it can phosphorylate tyrosine residues in mammalian cells [30]. In our experiments, we used the complex composed of two catalytic subunits (β) and two regulatory subunits (β) and succeeded in phosphorylating human centrins 1 and 2. HsCen1 was phosphorylated at one unique site, T138, which is surrounded by three acidic residues (D, E, E) based on the CK2 signature. The T138 residue is conserved among centrins, except for in human HsCen3 where it is replaced by a serine residue (Fig. 1). Because the S138 residue of HsCen3 is also surrounded by acidic residues, this site could still be a potential CK2 phosphorylation site. In contrast, C-HsCen2 was phosphorylated at both T138 and S158 residues. The S158 residue is also surrounded by two acidic E residues. However, this site is absent in human centrins HsCen1 and HsCen3, as well as in Cdc31 and centrin in *S. dubia*. Because HsCen1 is derived from a retrotransposition of HsCen2, the S158 residue most likely emerged after the appearance of HsCen1, and consequently, the N158 residue found at this position in other centrins is most likely the ancestral residue. An equivalent of the S158 residue of HsCen2 is found in primates as well as some fishes and birds (Fig. S6B).

The phosphorylation events of centrins 1 and 2 by CK2 as well as the co-localization of CK2 and centrin 1 and 2 in the connecting cilium have already been demonstrated [27]. However, several differences were observed between murine and human centrins. In mice, Cen1 and Cen2 are also phosphorylated at the T138 residue, although very weak phosphorylation of Cen3 has been observed. This is most likely due to the presence of R131, which could restrict CK2 from accessing the centrin, as we observed for K131 (Fig. S6A). Additionally, the S158 residue is absent in murine Cen2.

3.4. Phosphorylation by CK2 regulates the binding of human centrins to their targets (XPC, Sfi1 and transducin β

It was previously demonstrated that CK2-phosphorylation reduced the binding of murine centrins to transducin [27]. Our results showed that the CK2-phosphorylation of human centrin 1 completely abolished its ability to bind transducin β and reduced the binding of centrin 1 to other targets. In other studies, CK2-phosphorylation has the opposite consequences and enhances the binding of a protein to its target, as in the case of CLIP-170, which interacts with the kinetochore-microtubule upon CK2 phosphorylation [31].

The structure of transducin βγ in complex with phosducin has been solved by X-ray crystallography [32,24]. The transducin β residues that interact with phosducin are located outside of the centrin-binding site. However, the W332 residue of transducin β, which is part of the centrin-binding motif, establishes contacts with three residues (M101, H102 and L105) located in helix 3 of phosducin. Fig. S5 shows that the residues comprising the hydrophobic triad that binds centrin 1 are located in the last β-sheet at the C-terminus of transducin β. This clearly shows that the centrin-binding motif is completely embedded within the transducin

βγ–phosducin complex, with no way for centrin to reach its binding motif. Therefore, we believe that when phosducin interacts with transducin βγ, centrin cannot bind to transducin β.

Our experiments demonstrated that the binding of centrin to transducin is regulated by the phosphorylation of centrin. Additionally, the binding of phosducin to transducin is also regulated by phosphorylation. Phospho-phosducin, which is phosphorylated at S73 by PKA, cannot form a complex with transducin. Modeling experiments have shown that the phosphate group sterically and electrostatically clashes with the downstream residues in helix 2 particularly N75 and E76, thereby leading to the disruption of transducin αβγ binding.

3.5. Relationship between phosphorylation and Ca^{2+}-dependence of HsCen1 and HsCen2

For XPC, whose the binding to centrin is Ca^{2+}-independent, the phosphorylation at T138 has a little effect. However, the phosphorylation at S158, which exists in HsCen2, reduced the binding of XPC to HsCen2. Thus if HsCen2 is the natural isoform which binds XPC, phosphorylation at both T138 and S158 could regulate its binding to XPC. However, the double phosphomimetic T138D-S158D did not abolish the binding of HsCen2 to XPC, as there was a residual binding capacity of HsCen2 to XPC.

3.6. Phosphorylation of centrin could induce its conformational change

Conformational changes of phosphorylated proteins have been assessed using X-ray crystallography [33], NMR [34], hydrogen/deuterium exchange mass spectrometry (DXMS) [35] and molecular dynamics (MD) simulations [36].

Phosphorylation of a protein can either induce or prevent the binding of another molecule. Several examples have been reported in literature showing that phosphorylation of a protein induces the formation of complexes; here we report the results of four of these complexes. The first example concerns Elk-1, an eukaryotic transcription factor whose phosphorylation induces a conformational change that promotes its binding to DNA [37]. The second example involves Bcl-2, a central regulator in the mitochondrial-mediated apoptosis pathway. The phosphorylation of a disordered loop of Bcl-2 induces its conformational change and allows for consequent binding of Pin1 [38]. The third example concerns the *Staphylococcus aureus* protein VraR (a vancomycin-resistance-associated response regulator), whose phosphorylation promotes the dimerization of its DNA-binding domains [33]. X-ray crystal structures of VraR in both the unphosphorylated and beryllofluoride-activated state (which mimics the phosphorylated VraR) have been solved. The final example concerns the IIA-IIB complex of the N,N′-diacetylchitobiose transporter of the *Escherichia coli* phosphotransferase system which has been solved by NMR [34].

The phosphorylated residue can either be situated at the interface of the two partners or somewhere else in the protein. However, in the second case, the phosphorylation outside of the interface induces conformational changes, which consequently make that the target interface inaccessible to the binding partner.

Phosphorylation at the interface of the protein complex is illustrated by Erbin, which binds the C-terminus of the receptor tyrosine kinase ErbB2. The crystal structure of the PDZ domain Erbin in complex with an ErbB2-derived peptide, which contains a tyrosine residue, has been solved [39]. Phosphorylation of the ErbB2 tyrosine residue abolishes its binding to Erbin.

Two other examples illustrate the phosphorylation outside the interface of the partners. The first example concerns Cdc34-like enzymes, which catalyze the formation of polyubiquitin chains on several proteins [40]. Cdc34 contains an acidic loop whose conformation is modulated by CK2 phosphorylation of two residues S130 and S167. The authors analyzed other Cdc34-like enzymes and showed that there is a co-evolution of the phosphorylation sites and the acidic loop with regard to the proximity of the active site in Cdc34-like enzymes. Using multiple molecular dynamics (MD) simulations, the author investigated the conformational changes of the acidic loop which is characterized by a high conformational variability and some residues of the acidic loop were transiently close to the catalytic cleft. The authors hypothesized that phosphorylation of S130 situated outside of the acidic loop introduced a strong negatively charged group, which may result in electrostatic repulsion from the acidic loop. The second example concerns Rap1b, which is involved in the transduction of the cAMP-mitogenic response [35]. Rap1b is a GTPase that regulates the transduction of external stimuli. The S179 residue is situated at the extremity of a polybasic segment facing an acidic loop (D47 and E45), which connects 2 beta sheets also connected to the switch loops that interact with the nucleotide. The effect of the PKA-phosphorylation Ser179 on the conformational changes of Rap1 was analyzed using hydrogen/deuterium exchange mass spectrometry. Higher exchange was observed in both the phosphorylated and phosphomimetic state compared with the non-phosphorylated state of Rap1. Phosphorylation of S179 incorporates a repulsive negative charge that reflexively rotates the facing acidic loop and causes additional rotation of the switch loops.

In the case of centrin, CK2-phosphorylation also occurs outside the centrin hydrophobic cavity where the target protein normally binds. Based on the Cdc34 and Rap1 studies reported above, we propose a mechanism by which phosphorylation could regulate the binding capacity of the C-HsCen to its targets. Thus, phosphorylation of T138 could induce the repulsion of the acidic segment (E159, E160, E161) connected to the Ca^{2+} loop IV would consequently be oriented in such a way that it cannot bind calcium anymore. Furthermore, any Ca^{2+}-dependent regulation would effectively be eliminated.

4. Materials and methods

4.1. Chemicals, bacterial strains, plasmids

The peptides used in this study were purchased from GENECUST, and all the peptides were acetylated at their N-terminus and amidated at their C-terminus to increase their stability. Oligonucleotides were purchased from Eurogentec; dNTPs, *NdeI* and *XhoI* restriction enzymes, T4 DNA ligase, and Finnzymes Phusion DNA polymerase were purchased from New England Biolabs. The pET24 vector and *E. coli* NM554 and Bl-21(DE3) strains were purchased from Novagen. DEAE-TSK and phenyl-TSK were purchased from Interchim. Sephadex G25 was purchased from GE-Healthcare.

4.2. Cloning of human centrins 1, 2 and site-directed mutagenesis

The human centrin 1 coding sequence was amplified from a clone (a gift from Bornens) via polymerase chain reaction (PCR) using Phusion DNA polymerase, dNTPs, and the flanking primers 5′-C1 (5′-GGAATTCCATATGGCTTCCGGCTTCAAGAAG-3′) and 3′-C1 (5′-CGGCGCTCGAGTCAGTAAAGGCTGGTCTTCTTCAT-3′) to create plasmid pLA11.33.2 encoding full-length centrin 1. Site-directed mutagenesis was accomplished via the double PCR method [41], using a wild type clone as the template, containing dNTPs, and Phusion DNA polymerase both flanking 5′- and 3′-primers listed above and the following mutagenic oligonucleotides: for pLA11.33.20 encoding Cen1-T138D 3′-C1T138D (5′-CTGCAGCTCC TCATCATCGAGGTTCTCCCCCAG-3′); for pLA11.33.38 encoding Cen1-T138E 3′-C1T138E (5′-CTGCAGCTCCTCATCTTCGAGGTTCTC CCCCAG-3′); for pLA11.33.25 encoding Cen1-N131K 3′-C1N131K

(5′-GTTCTCCCCCAGCTCCTTGGCCACACGCTTCAG-3′). The C-terminal domain of centrin 1 (wild type and variants) was generated using the above plasmids (full-length) and the flanking primers, 5′-C1M93 (5′-GGAATTCCATATGACGCAGAAGATGTCCGA-3′) or 5′-C1M97 (5′-GGAATTCCATATGTCCGAGAAGGACACCAAAGAAG-3′) and 3′-C1, resulting in the following plasmids: pLA11.33.23 (C-Cen1-M93-Y172), pLA11.33.5 (C-Cen1-M97-Y172), pLA11.33.32 (C-Cen1-T138D), pLA11.33.39 (C-Cen1-T138E), and pLA11.33.25 (C-Cen1-N131K).

Full-length centrin 2 and the C-terminal domain (M93-Y172) were obtained from [19]. Site-directed mutagenesis of centrin 2 was accomplished as above using centrin 2 wild-type full-length and flanking primers 5′-C2 (5′-GGAATTCCATATGGCCTCCAACTT TAAGAAGG-3′), 3′-C2 (5′-CGGCGCTCGAGTTAATAGAGGCTGGTCTT TTTCAT-3′), and 3′- primers listed above and the following mutagenic oligonucleotides: for pLA11.37.12 encoding Cen2-K131N 3′-C2K131N (5′-GTTCTCACCCAACTCGTTGGCCACGCGTTTCAG-3′), for pLA11.37.8 encoding C2T138D 3′-C2T138D:5′-CTGCAGCTCCTCATC ATCCAGGTTCTCACCCAA-3′; for pLA11.37.13 encoding C2T138A 3′-C2T138A: 5′-CTGCAGCTCCTCATCAGCCAGGTTCTCACCCAA-3′; for pLA11.37.14 encoding C2S158D 3′-C2S158D: 5′-CAGGAACTCTTGC TCATCGACCTCTCCATCTCC-3′; for pLA11.37.15 encoding C2S158A 3′-C2S158A: 5′-CAGGAACTCTTGCTCAGCGACCTCTCCATCTCC-3′; for pLA11.37.28 encoding C2T138D-S158D, pLA11.37.14 encoding C2S158D was used as template with 3′-C2T138D mutagenic oligonucleotide.

The C-terminal domain of all centrin 2 mutants were generated by PCR using the above plasmids (full-length) mutants as templates and the flanking primers 5′-C2M93 5′-GGAATTCCATATGACC CAGAAAATGTCTGAGAAA-3′ and 3′-C2 resulting in the following plasmids: pLA11.37.17 (encoding C-Cen2-K131N), pLA11.37.18 (encoding C-C2-T138D), pLA11.37.30 (encoding C-Cen2-T138A), pLA11.37.19 (encoding C-C2-S158D), pLA11.37.20 (encoding C-Cen2-S158A), pDAG1.1.1 (encoding C-C2-T138D-S158D), pLA11.37.32 (encoding C-Cen2T138A-S158A).

All the PCR products were digested with the *NdeI* and *XhoI* restriction enzymes, and T4 DNA ligase was used to insert the mutated genes between the *NdeI* and *XhoI* restriction sites of the pET24a expression vector. The resulting plasmids were used to transform the *E. coli* NM554 strain, and the transformed clones were sequenced to verify their integrity and the incorporation of the desired mutation. DNA from successfully transformed clones was isolated and used to transform *E. coli* strain BL21(DE3)/pDIA17 cells, which are chloramphenicol resistant, in order to express the recombinant proteins.

4.3. Expression and purification of human centrins 1, 2 from E. coli

To overproduce centrins 1 and 2, bacteria containing plasmids, were grown at 37 °C in 2YT medium (Difco) supplemented with chloramphenicol (30 μg/mL) and kanamycin (70 μg/mL). When an OD_{600} of 1.5, was reached, protein production was induced with 1 mM isopropyl-β-D-1-thiogalactopyranoside (IPTG), and the cell were to grow for an additional 3 h at 37 °C. The cells were then pelleted by centrifugation and served as a protein purification source.

The extracts were heated at 63 °C for 10 min, and the denatured proteins were removed by centrifugation. Because the isoelectric points of all the proteins ranged from 4.35 to 4.91, the same protocol was used to purify all of them. Centrins 1, 2, and their variants (full-length and C-terminal domains) were purified using three successive chromatographic steps including DEAE-TSK (ion exchange), phenyl-TSK (reversed phase) and G25 (gel filtration). Centrins were then lyophilized, and the degree of purity was assessed using SDS–PAGE. Centrin concentration was determined using UV absorption spectrophotometry at 280 nm using the standard molar absorption coefficient (E_M) of 1490 $M^{-1}cm^{-1}$ (1 residue tyrosine) for the full-length centrin or at 258 nm using the standard molar absorption coefficient (E_M) of 1000 $M^{-1}cm^{-1}$ (5 residues phenylalanine) for the C-terminal domains.

4.4. In vitro phosphorylation of human centrins 1 and 2 by CK2

Samples of 250 μM centrin (wild type or variants) were phosphorylated using 1000 units of CK2 (Casein kinase II is composed of two 44 kDa catalytic α-subunits and two 26 kDa regulatory β-subunits; specific activity 859,000 units per mg) in 1 mL of Buffer (50 mM Tris–HCl pH 7.5, 2 mM ATP, 10 mM $MgCl_2$, 100 mM NaCl, 0.02% NaN_3) in the absence or presence of 2 mM $CaCl_2$ and 1 mM EGTA. The incubation was carried out at 37 °C for 40 h. Aliquots (33 μL) were removed from the sample and immediately placed in nitrogen liquid to stop the phosphorylation reaction. The aliquots were kept at −20 °C until HPLC analysis. A 10 μL aliquot from the kinetic sample was added to 90 μL water and analyzed on a DEAE-TSK 5PW column using HPLC. Phosphorylated and unphosphorylated centrins were separated using a linear gradient of 35–65% buffer B (40 mM NaH_2PO_4 – 0.4 M NaCl, pH 7.86) completed with buffer A (40 mM NaH_2PO_4 pH 7.86). Proteins and phosphorylated proteins were detected at 210 nm and 280 nm. The ratio of phosphorylated and to non-phosphorylated proteins was determined by the integration of peaks using the program System Gold (version 1990). The determination of phosphorylated residues was assessed using MALDI-TOF mass spectrometry on tryptic fragments of both C-HsCentrins 1 and 2.

All proteins (wild type and variants) were first tested for their stability in buffer (50 mM Tris–HCl pH 7.5, 10 mM $MgCl_2$, 100 mM NaCl, 0.02% NaN_3) at 37 °C for 40 h, in the presence or absence of 2 mM $CaCl_2$.

4.5. Isothermal titration calorimetry (ITC)

The thermodynamic parameters of the molecular interactions between human centrins (full-length 1 and 2 and their C-terminal domains) and the target peptide were investigated via ITC using a MicroCal MCS instrument (MicroCal Inc., Northampton, MA). The protein and peptide were equilibrated in the same buffer (50 mM MOPS, 100 mM NaCl pH 7.5) supplemented with 1 mM $CaCl_2$ or 2 mM EDTA. The centrins (10 μM) in the calorimeter cell were titrated with the peptide-target (100 μM) by automatic injections of 8–10 μL at 30 °C. On some occasions, the centrin/peptide target ratio was 10–170 μM. The first injection of 2 μL was ignored in the final data analysis. Integration of the peaks corresponding to each injection and correction for the baseline were performed using the Origin-based software provided by the manufacturer. The data were fitted to an interaction model to generate the stoichiometry (n), equilibrium binding constant (K_a), and enthalpy of complex formation (ΔH). Control experiments consisting of injections of the peptide solution into the buffer were performed to evaluate the heat of dilution.

4.6. Bioinformatics

Calculations of pI and PM were made using Expasy resources. Multiple sequences alignments were performed using the ClustalW program.

Acknowledgements

This work was supported by the Centre National de la Recherche Scientifique, the Institut National de la Santé et de la Recherche Médicale and the Institut Curie. Dora Grecu acknowledges a PhD Grant from the Université Pierre et Marie Curie. We thank the Laboratoire de Spectrométrie de Masse Protéomique de l'Institut Curie.

Appendix A. Supplementary data

Supplementary data associated with this article can be found, in the online version, at http://dx.doi.org/10.1016/j.fob.2014.04.002.

References

[1] Salisbury, J.L., Baron, A., Surek, B. and Melkonian, M. (1984) Striated flagellar roots: isolation and partial characterization of calcium-modulated organelle. J. Cell Biol. 99, 962–970.

[2] Huang, B., Mengersen, A. and Lee, V.D. (1988) Molecular cloning of cDNA for caltractin, a basal body-associated Ca^{2+}-binding protein: homology in its sequence with calmodulin and the yeast CDC31 gene product. J. Cell Biol. 107, 133–140.

[3] Hart, P.E., Glantz, J.N., Orth, J.D., Poynter, G.M. and Salisbury, J.L. (1999) Testis-specific murine centrin, Cetn1: genomic characterization and evidence for retroposition of a gene encoding a centrosome protein. Genomics 60, 111–120.

[4] Friedberg, F. (2006) Centrin isoforms in mammals. Relation to calmodulin. Mol. Biol. Rep. 33, 243–252.

[5] Gavet, O., Alvarez, C., Gaspar, P. and Bornens, M. (2003) Centrin4p, a novel mammalian centrin specifically expressed in ciliated cells. Mol. Biol. Cell 14, 1818–1834.

[6] Paoletti, A., Moudjou, M., Paintrand, M., Salisbury, J.L. and Bornens, M. (1996) Most of centrin in animal cells is not centrosome-associated and centrosomal centrin is confined to the distal lumen of centrioles. J. Cell Sci. 109, 3089–3102.

[7] Spang, A., Courtney, I., Fackler, U., Matzner, M. and Schiebel, E. (1993) The calcium-binding protein cell division cycle 31 of *Saccharomyces cerevisiae* is a component of the half bridge of the spindle pole body. J. Cell Biol. 123, 405–416.

[8] Wolfrum, U. and Salisbury, J.L. (1998) Expression of centrin isoforms in the mammalian retinae. Exp. Cell Res. 242, 10–17.

[9] Araki, M., Masutani, C., Takemura, M., Uchida, A., Sugawasa, K., Kondoh, J., Ohkuma, Y. and Hanaoka, F. (2001) Centrosome protein centrin 2/caltractin 1 is part of he xeroderma pigmentosum group C complex that initiates global genome nucleotide excision repair. J. Biol. Chem. 276, 18665–18672.

[10] Kilmartin, J.V. (2003) Sfi1p has conserved centrin-binding sites and an essential function in budding yeast spindle pole body duplication. J. Cell Biol. 162 (7), 1211–1221.

[11] Jani, D., Lutz, S., Marshall, N.J., Fisher, T., Köhler, A., Ellisdon, A.M., Hurt, E. and Stewart, M. (2009) Sus1, Cdc31, and the Sac3 CDI region form a conserved interaction platform that promotes nuclear pore association and mRNA export. Mol. Cell. 33, 727–737.

[12] Baum, P., Furlong, C. and Byers, B. (1986) Yeast gene required for spindle pole body duplication: homology of its product with Ca^{2+}-binding proteins. Proc. Natl. Acad. Sci. U.S.A. 83, 5512–5516.

[13] Puvermüller, A., Giessl, A., Heck, M., Wottrich, R., Schmitt, A., Ernst, O.P., Choe, H.W., Hofmann, K.P. and Wolfrum, U. (2002) Calcium dependent assembly of centrin/G-protein complex in photoreceptor cells. Mol. Cell Biol. 22, 2194–2203.

[14] Giessl, A., Pulvermuller, A., Trojan, P., Park, J.H., Choe, H.W., Ernst, O.P., Hofmann, K.P. and Wolfrum, U. (2004) Differential expression and interaction with the visual G-protein transducin of centrin isoforms in mammalian photoreceptor cells. J. Biol. Chem. 279, 51472–51481.

[15] Thompson, J.R., Ryan, Z.C., Salisbury, J.L. and Kumar, R. (2006) The structure of the human centrin2-xeroderma pigmentosum group C protein complex. J. Biol. Chem. 281, 18746–18752.

[16] Charbonnier, J.B., Renaud, E., Miron, S., Le Du, M.H., Blouquit, Y., Duchambon, P., Christova, P., Shosheva, A., Rose, T., Angulo, J.F. and Craescu, C.T. (2007) Structural, thermodynamic and cellular characterization of human centrin 2 interaction with xeroderma pigmentosum group c protein. J. Mol. Biol. 373, 1032–1046.

[17] Li, S., Sandercock, A.M., Conduit, P., Robinson, C.V., Williams, R.L. and Kilmartin, J.V. (2006) Structural role of Sfi1p-centrin filaments in budding yeast spindle pole duplication. J. Cell Biol. 173, 867–877.

[18] Matei, E., Miron, S., Blouquit, Y., Duchambon, P., Durussel, I., Cox, J.A. and Craescu, C.T. (2003) The C-terminal half of human centrin 2 behaves like a regulator EF-hand domain. Biochemistry 42, 1439–1450.

[19] Yang, A., Miron, S., Mouawad, L., Duchambon, P., Blouquit, Y. and Craescu, C.T. (2006) Flexibility and plasticity of human centrin 2 binding to the protein XPC from nuclear excision repair. Biochemistry 45, 3645–3663.

[20] Martinez-Sanz, J., Kateb, F., Assairi, L., Blouquit, Y., Bodenhausen, G., Abergel, D., Mouawad, L. and Craescu, C.T. (2010) Structure, dynamics and thermodynamics of the human centrin 2/hSfi1 complex. J. Mol. Biol. 395, 191–204.

[21] Giessl, A., Trojan, P., Raush, S., Pulvermüller, A. and Wolfrum, U. (2006) Centrins, gatekeepers for the light-dependent translocation of transducin through the photoreceptor cell connecting cilium. Vision Res. 46, 4502–4509.

[22] Bauer, P.H., Muller, S., Puzicha, M., Pippig, S., Obermaier, B., Helmreich, E.J.M. and Lohse, M.J. (1992) Phosducin is a protein kinase A-regulated G protein regulator. Nature 358, 73–76.

[23] Danner, S. and Lohse, M.J. (1996) Phosducin is a ubiquitous G protein regulator. Proc. Natl. Acad. Sci. U.S.A. 93, 10145–10150.

[24] Gaudet, R., Bohm, A. and Sigler, P.B. (1996) Crystal structure at 2.4 Å resolution of the complex of transducin βγ and its regulator, phosducin. Cell 87, 577–588.

[25] Loew, A., Ho, Y.K., Blundell, T. and Bax, B. (1998) Phosducin induces a structural change in transducin βγ. Structure 6, 1007–1019.

[26] Gaudet, R., Savage, J.R., McLaughlin, J.N., Willardson, B.M. and Sigler, P.B. (1999) Mol. Cell. 3, 649–660.

[27] Trojan, P., Raush, S., Giessl, A., Klemm, C., Krause, E., Pulvermüller, A. and Wolfrum, U. (2008) Light-dependent CK2-mediated phosphorylation of centrins regulates complex formation with visual G-protein. Biochem. Biophys. Acta 1783, 1248–1260.

[28] Thissen, M.C., Krieglstein, J., Wolfrum, U. and Klumpp, S. (2009) Dephosphorylation of centrins by phosphatase 2C α and β. Res. Lett. Biochem. 2009, 685342.

[29] Grecu, D., Blouquit, Y. and Assairi, L. (2013) The E144 residue of *Scherffelia dubia* discriminates between the DNA repair protein XPC and the centrosomal protein Sfi1. FEBS 4, 33–42.

[30] Vilk, G., Weber, J.E., Duncan, J.S., Wu, C., Derksen, D.R., Zien, P., Sarno, S., Donella-Deana, A., Lajoie, G., Pinna, L.A., Li, S.S. and Lichfield, D.W. (2008) Protein kinase CK2 catalyzes tyrosine phosphorylation in mammalian cell. Cell Signal 20 (11), 1942–1951.

[31] Li, H., Liu, X.S., Yang, X., Wang, Y., Wang, Y., Turner, J.R. and Liu, X. (2010) Phosphorylation of CLIP-170 by Plk1 and CK2 promotes timely formation of kinetochore-microtubule attachments. EMBO J. 29, 2953–2965.

[32] Gaudet, R., Bohm, A. and Sigler, P.B. (1996) Crystal structure at 2.4Å resolution of the complex of transducin βγ and its regulator, phosducin. Cell 87, 577–588.

[33] Leonard, P.G., Golemi-Kotra, D. and Stock, A.M. (2013) Phosphorylation-dependent conformational changes and domain rearrangements in *Staphylococcus aureus* VraR activation. Proc. Natl. Acad. Sci. U.S.A. 110, 8225–8530.

[34] Jung, Y.-S., Cai, M. and Clore, G.M. (2010) Solution structure of the $IIA^{chitobiose}$–$IIB^{chitobiose}$ complex of the N,N′-diacetylchitobiose branch of the *Escherichia coli* phosphotransferase system. J. Biol. Chem. 285, 4173–4184.

[35] Edreira, M.M., Li, A., Hochbaum, D., Wong, S., Gorfe, A.A., Ribeiro-Neto, F., Woods, V.L. and Altshuler, D.L. (2009) Phosphorylation-induced conformational changes in Rap1b allosteric effects on switch domains and effector loop. J. Biol. Chem. 284, 27480–27486.

[36] Groban, E., Narayanan, A. and Jacobson, M. (2006) Conformational changes in protein loops and helices induced by post-translational phosphorylation. PLOS Comput. Biol. 2 (4), e32.

[37] Yang, S.-H., Shore, P., Willingham, N., Lakey, J.H. and Sharrocks, A.D. (1999) The mechanism of phosphorylation-inducible activation of the ETS-domain transcription factor Elk-1. EMBO J. 18, 5666–5674.

[38] Kang, C.B., Bharatham, N., Chia, J., Mu, Y., Baek, K. and Yoon, H.S. (2012) The natively disordered loop of Bcl-2 undergoes phosphorylation-dependent conformational change and interacts with Pin1. PLoS One 7 (12), e52047.

[39] Birrane, G., Chung, J. and Ladias, J.A.A. (2003) Novel mode of ligand recognition by the Erbin PDZ domain. J. Biol. Chem. 278, 1399–1402.

[40] Papaleo, E., Ranzani, V., Tripodi, F., Vitriolo, A., Cirulli, C., Fantucci, P., Alberghina, L., Vanoni, M., De Gioia, L. and Coccetti, P. (2011) An acidic loop and cognate phosphorylation sites define a molecular switch that modulates ubiquitin charging activity in Cdc34-like enzymes. PLOS Comput. Biol. 7 (5), e1002056.

[41] Picard, V. and Bock, S.C. (1997) Rapid and efficient one-tube PCR-based mutagenesis method. Methods Mol. Biol. 67, 183–188.